Tuning the Superstructure of Ultrahigh-Molecular-Weight Polyethylene/Low-Molecular-Weight Polyethylene Blend for Artificial Joint Application

Ling Xu,[†] Chen Chen,*[,‡] Gan-Ji Zhong,[†] Jun Lei,[†] Jia-Zhuang Xu,[†] Benjamin S. Hsiao,[§] and Zhong-Ming Li*[,†]

[†]College of Polymer Science and Engineering and State Key Laboratory of Polymer Materials Engineering and [‡]Analytical and Testing Center, Sichuan University, Chengdu 610065, China

[§]Department of Chemistry, Stony Brook University, Stony Brook, New York 11794-3400, United States

Ⓢ *Supporting Information*

ABSTRACT: An easy approach was reported to achieve high mechanical properties of ultrahigh-molecular-weight polyethylene (UHMWPE)-based polyethylene (PE) blend for artificial joint application without the sacrifice of the original excellent wear and fatigue behavior of UHMWPE. The PE blend with desirable fluidity was obtained by melt mixing UHMWPE and low molecular weight polyethylene (LMWPE), and then was processed by a modified injection molding technology-oscillatory shear injection molding (OSIM). Morphological observation of the OSIM PE blend showed LMWPE contained well-defined interlocking shish-kebab self-reinforced superstructure. Addition of a small amount of long chain polyethylene (2 wt %) to LMWPE greatly induced formation of rich shish-kebabs. The ultimate tensile strength considerably increased from 27.6 MPa for conventional compression molded UHMWPE up to 78.4 MPa for OSIM PE blend along the flow direction and up to 33.5 MPa in its transverse direction. The impact strength of OSIM PE blend was increased by 46% and 7% for OSIM PE blend in the direction parallel and vertical to the shear flow, respectively. Wear and fatigue resistance were comparable to conventional compression molded UHMWPE. The superb performance of the OSIM PE blend was originated from formation of rich interlocking shish-kebab superstructure while maintaining unique properties of UHMWPE. The present results suggested the OSIM PE blend has high potential for artificial joint application.

KEYWORDS: ultrahigh-molecular-weight polyethylene (UHMWPE), flow-induced polymer orientation and crystallization, tuning morphology and superstructure, mechanical properties, artificial joints
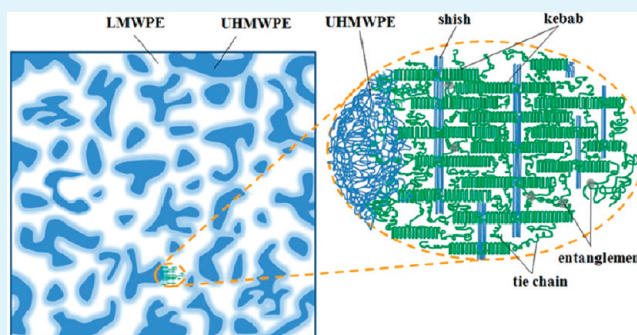
INTRODUCTION

The special composite microstructure of UHMWPE, whose quite long, regular, and nonpolar molecular chains always connect different lamellae through the amorphous phase, endows it with superior properties, such as outstanding mechanical properties, very low friction and wear rate, excellent fatigue resistance as well as recognized biocompatibility.[1] UHMWPE has hence been extensively used for decades as the material of load-bearing, articulating surface for the metal/articular pair in total joint arthroplasty.[2] Despite its enormous success in implant surgery, bone resorption around the implants (peri-prosthetic osteolysis) secondary to UHMWPE wear debris generated during in vivo use occurred frequently,[3,4] limiting the long-term performance of total joints and necessitating revision surgery. Radiation cross-linking by high dose irradiation was proposed to improve the wear behavior of UHMWPE implants, which was proved to benefit to wear resistance.[5–7] However, radiation also leaves behind long-lived residual free radicals, which can cause oxidation in the long

term and also detrimentally affect mechanical properties, such as a decrease in ultimate tensile strength, ductility, toughness and fatigue resistance.[8–12] As reported, addition of antioxidant (such as vitamin E) can effectively increase oxidation stability to prevent oxidation of UHMWPE,[13] but it cannot yet make up for the loss of mechanical properties.[14] This limits the applications of UHMWPE implants in the case of high stress such as total knee implants, especially in younger and more physically active patients. It can therefore be drawn the conclusion that the damage to UHMWPE in vivo caused by either wear debris, oxidation or mechanical performance degradation is a crucial factor that adversely affects the long-term performance of the reconstructed joint. Inspiringly, improvement of wear resistance and oxidation stability of UHMWPE has achieved satisfying success as described above.
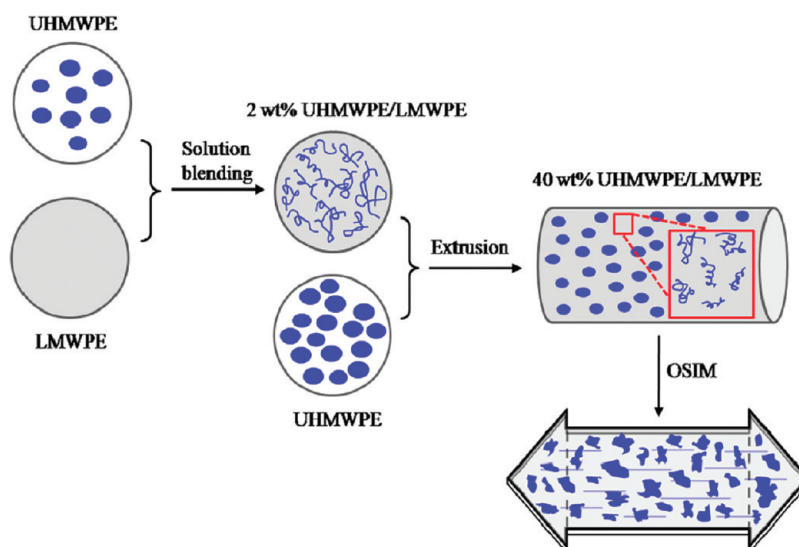
Figure 1. Sketch of the processing procedures.

The current challenge is how to enhance mechanical properties of the UHMWPE implants without sacrifice of wear resistance and oxidation stability.

Efficiency of fabrication of UHMWPE implants is another challenge. Because of its ultrahigh molecular weight, the exceptionally high melt viscosity of UHMWPE leads to a gel state, making it nearly impossible to be processed by up-to-date polymer processing technologies such as screw extrusion, injection molding, etc. Currently, only compression molding (CM) and ram extrusion can be adopted to consolidate UHMWPE resins,[15] whereas during these processing procedures, UHMWPE resins have to stay at high temperature for a long time (about 200 °C for at least two hours) to completely melt and finally consolidate.[16] Unfortunately, this process takes some risks damaging the performance of UHMWPE parts: First, long-time exposure at high temperature could cause molecular chain scission and oxidization, leading to performance deterioration of joint implants, and also generate free radicals during degradation, which is potentially harmful for the health of patient.[17,18] Second, the boundaries of UHMWPE particles with extremely low diffusion coefficient are not thoroughly erased due to inefficient compounding. Structural defects may be induced by the incomplete welding of boundaries, making joint implants easy to rupture, especially under a severe motion of joints.[19] As far as we know, by utilizing conventional processing methods, compounding force can be provided to effectively and substantially mix polymer melt in quite short time at a relatively low temperature, avoiding the aforementioned disadvantages. But, as for conventional processing methods, good fluidity of materials is the prerequisite, which is exactly the difficulty for UHMWPE and hardly overcome up to now.[20]

To process UHMWPE under flow field, the problem of its liquidity needs to be first solved. Polymer blending is a versatile way to improve processability of UHMWPE. Blending low-molecular-weight polyethylene (LMWPE) with UHMWPE could be a desirable method because both biocompatibility and interface adhesion are not sacrificed.[21,22] However, the deterioration of mechanical properties of UHMWPE due to the simple addition of LMWPE has not been resolved yet.[23–26] Therefore, enhancement of mechanical properties while achieving improved processing performance is becoming the

key for UHMWPE to be a successful joint replacement material. It is well-established that the formed superstructures in polymer blend often dictate the subsequent development of morphology and thus the final properties.[12] Accordingly, properly tailoring microstructures, especially inducing formation of some unique superstructure, could be a solution to improve mechanical properties of joint implants. Generation of self-reinforced structure, e.g., shish-kebab superstructure, which can be achieved through taking advantage of flow field is a preferred option on such a lot substantial theoretical basis.[27–29] Also, many studies confirmed that the high-molecular-weight species (such as UHMWPE) facilitate the efficient formation of shish-kebabs in the entangled melt under a given flow condition.[30–36] The long chains of UHMWPE can be stretched under shear or elongational flow fields in melts and crystallize into shish and the coiled chains are subsequently adsorbed onto the shish and form kebabs.[31] Unfortunately, shish-kebab superstructure is actually a kind of oriented structure which generally enhances mechanical properties of products in one direction significantly and hardly affects these in other directions.[37–39] Therefore, the goal of achieving balanced performance of joint parts in each direction is of high significance.

In this work, UHMWPE was blended with LMWPE aiming to obtain PE blend with desirable fluidity, and then UHMWPE/LMWPE blend was processed under oscillation shear stress field to form shish-kebab superstructure with the intention of achieving suitable artificial joint specimens with superior comprehensive performance. The oscillation shear stress field imposed on polymer melt was provided by means of hydraulically actuated pistons equipped on a modified injection molding machine, i.e., oscillatory shear injection molding (OSIM) whose picture is available in the Supporting Information (Figure S1 and S2). Oscillatory shear injection molded UHMWPE/LMWPE blend samples (OSIM PE blend) are successfully prepared and well-characterized. To obtain rich shish-kebab self-reinforcement structure, a small amount of UHMWPE was added into LMWPE through solution blending to act as the precursor of shish-kebabs. The results show that there are a large amount of interlocking shish-kebab superstructure formed in the OSIM PE blend, and compared to conventional compression molded UHMWPE (CM

UHMWPE), tensile and impact strength of the OSIM PE blend were significantly enhanced without sacrificing the original excellent wear and fatigue behavior of CM UHMWPE.

■ EXPERIMENTAL SECTION

Materials. The chosen LMWPE was supplied by the Dow Chemical Company, with a melt flow rate (MFR) of 20 g/10 min (190 °C, 21.6 N), M_w = 1.2 × 10^5 g/mol. UHMWPE powder (M_v = 5.5 × 10^6 to 6.0 × 10^6 g/mol) was provided by Second Auxiliary Factory, Beijing, China.

Preparation of Oscillatory Shear Injection Molding PE Blend (OSIM PE Blend) and Compression Molded Neat UHMWPE (CM UHMWPE). *OSIM PE Blend.* Two weight percent UHMWPE powder, which was significantly higher than the estimated overlap concentration of UHMWPE (c^* ≈ 0.2 wt %),[40] was first mixed with LMWPE by a solution blending procedure to ensure that the two species were intimately mixed at the molecular level. The above polymer blend was used as a master batch. The master batch was then melt mixed with UHMWPE powder in a twin-screw extruder to produce pellet samples containing 40 wt % UHMWPE. The processing temperature profile was limited within 160−190 °C from hopper to die, and the screw speed was fixed at 80 rpm. The pellets were initially injected into a dumbbell mold in a temperature profile of 170−200 °C from hopper to nozzle. Subsequently, the oscillation shear provided by the OSIM machine is continuously imposed on the melt. Sketch of the processing procedures mentioned above is shown in Figure 1. Generally, the OSIM can provide a peak shear rate in a single cycle from several per second up to hundreds per second, which is set to be about 220 s^{-1} in this work. The main feature of OSIM is that microstructure of polymer can be modulated and well-controlled by the particular "melt manipulation" processing, which does not exist in other processing methods.[29]

CM UHMWPE. For comparison, the conventional compression molded UHMWPE were employed as the control sample. UHMWPE powder was pressurized to 15 MPa and stayed at 150 °C for 2 h to be compression molded into 22 × 10 × 5 cm^3 blocks.[16] The testing samples were machined from the blocks.

Mechanical Testing. Tensile properties of the dumbbell samples parallel and perpendicular to shear flow direction were measured using the Instron Instrument model 5576 according to ASTM D-638 at a cross-head speed of 10 mm/min. Notched Izod impact strength of CM UHMWPE and OSIM PE blend samples was carried out according to the standard GB/T 1843−96. Five specimens were tested, and the average value was reported. Rheological behavior of the samples was also characterized (see Figure S3 in the Supporting Information).

Wear Testing. Wear behavior was evaluated using MM-200 wear tester (Xuanhua Testing Machine Factory, Hebei CITY, China). The specimens slide against GCr15 stainless steel, on which CoCr coating (Ra = 0.02 μm) was prepared, with a block-on-ring contact, providing a contact normal force of 200 ± 0.2 N. The schematic diagram of the wear tester is showed in Figure 2. The block specimens are of size 30
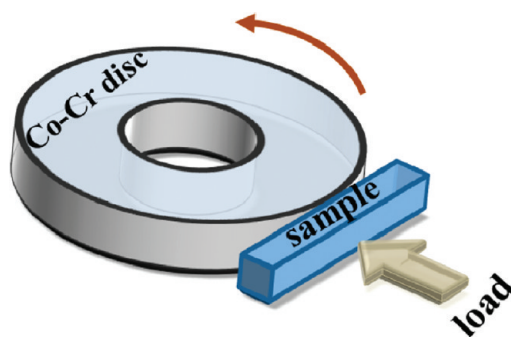
mm × 7 mm × 4 mm. The diameter of the counterpart steel ring is 40 mm. The tests were carried out at a linear velocity of 0.43 m/s, ambient temperature around 25 °C and one revolution were regarded as a cycle. Wear rate was calculated as the linear regression of weight loss versus number of cycles from 0.5 MC to 1 MC. Three test specimens of each sample were tested.

Fatigue Crack Propagation Testing. Fatigue crack propagation tests were performed following ASTM E-647. Compact tension (C(T)) specimens (n = 3) were precracked at the notch using a razor blade. Testing was conducted at a sinusoidal load cycle frequency of 5 Hz and stress ratio of 0.1 in tension. Crack length was monitored optically every 20 000 cycles. The average of the crack length on both sides of the C(T) specimen was used as the representative crack length for the computation of crack growth rates. Stress intensity factor ranges at crack inception (ΔK_i) were reported in MPam$^{1/2}$ at a threshold crack growth rate of 1 × 10^{-6} mm/cycle. All testing was done in an aqueous bath at 40 °C to simulate the physiologic temperature of the joint.

Morphology Observation with Scanning Electron Microscopy (SEM). The test specimen were cryogenically fractured in liquid nitrogen, and etched by 1% solution of potassium permanganate in a mixture of sulphuric acid, 85% orthophosphoric acid and water.[41] Then the etched surface was covered with a thin layer of gold and observed by a SEM instrument (Inspect F, FEI Company) operating at 20 kV. To investigate the detailed microstructure, the samples are divided into outer and inner layers, which are referred to the layers from surface to ca. 1.0 mm deep and from 1.0 to ca. 2.0 mm (the total depth is 4.0 mm), respectively.

Thermal Analysis by Differential Scanning Calorimetry (DSC). A Perkin-Elmer diamond-II differential scanning calorimetry (DSC) was used to determine the melting and crystallization behaviors of the specimen. Detailed procedures were set as follows: (a) the samples mentioned (approximately 5 mg) were weighed and placed in aluminum sample pans. (b) The pan was crimped with an aluminum cover. (c) The samples were then heated from 40 to 180 °C at a heating rate of 10 °C/min under nitrogen purge. Heat flow as a function of time and temperature was recorded. Crystallinity of the samples (n = 3 each) was determined by integrating the enthalpy peak from 40 to 160 °C, and normalizing it with the enthalpy of melting of 100% crystalline polyethylene, 291 J/g.

Determination of Crystal Structure by WAXD and SAXS. Two-dimensional wide-angle X-ray diffraction (2D-WAXD) and small-angle X-ray scattering (SAXS) were used to characterize the crystalline structure and molecular orientation distribution along the sample width direction. WAXD and SAXS measurements were carried out at the Advanced Polymers Beamline (X27C, λ = 1.371 Å) in the National Synchrotron Light Source (NSLS), Brookhaven National Laboratory (BNL). A MAR CCD X-ray detector (MARUSA) was employed for detection of 2D-WXAD and 2D-SAXS images, having a resolution of 1024 × 1024 pixels (pixel size = 158.44 μm). The data acquisition time was 180 s for each scattering pattern (image). The sample to detector distance was 112.6 and 2330 mm for WAXD (calibrated by an aluminum oxide (Al$_2$O$_3$) standard) and SAXS (calibrated by a silver behenate (AgBe) standard), respectively. The Fit-2D software package was used to analyze the 2D WAXD and SAXS patterns. For evaluation of molecular orientation, the orientation parameter was calculated mathematically using Picken's method from the (110) reflection of WAXD for PE.[42]

■ RESULTS

The mechanical properties of OSIM PE blend are summarized in Figure 3. In comparison with the CM UHMWPE, the OSIM PE blend exhibits remarkable improvement of ultimate tensile strength (Figure 3a) and impact strength (Figure 3d) along the direction of shear flow. It is truly amazing to find that the mechanical properties in the transverse direction are also more or less increased. Thus, it is reasonable to deduce the OSIM PE blend does not just contain the conventional shish−kebab self-reinforced superstructure, since the oriented structure is
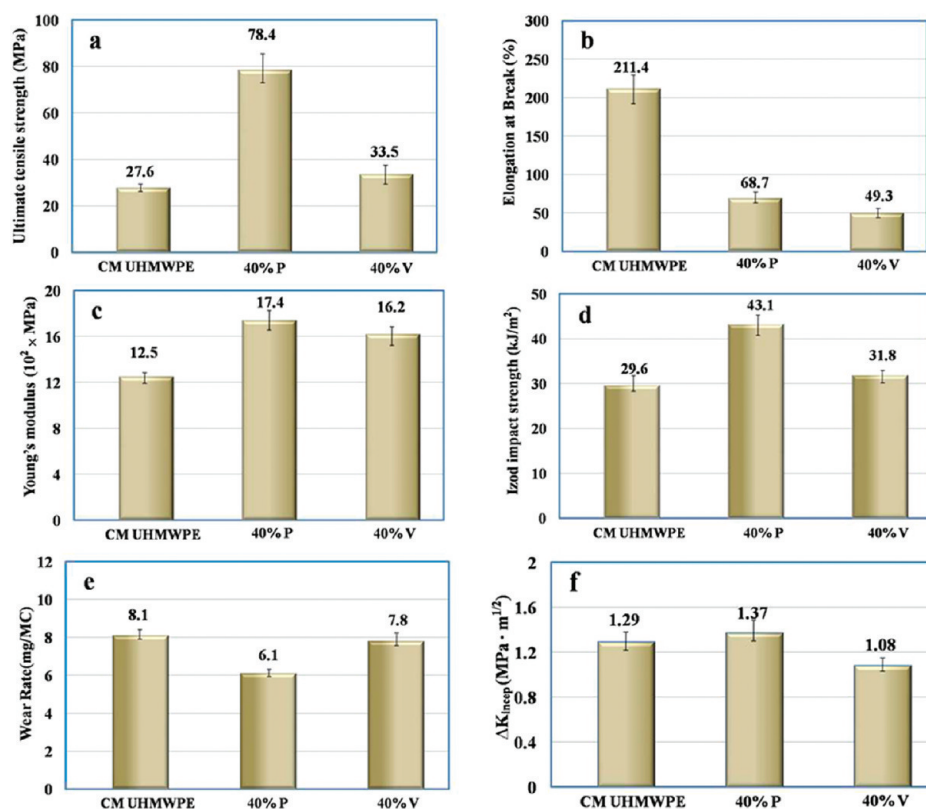

Figure 2. Schematic diagram of frictional pair contact.

Figure 3. (a)Ultimate tensile strength, (b) elongation at break, (c) Young's modulus, (d) Izod impact strength, (e) wear rate, (f) fatigue crack propagation resistance of CM UHMWPE and OSIM PE blend parallel (40%P) and vertical (40%V) to the flow direction.
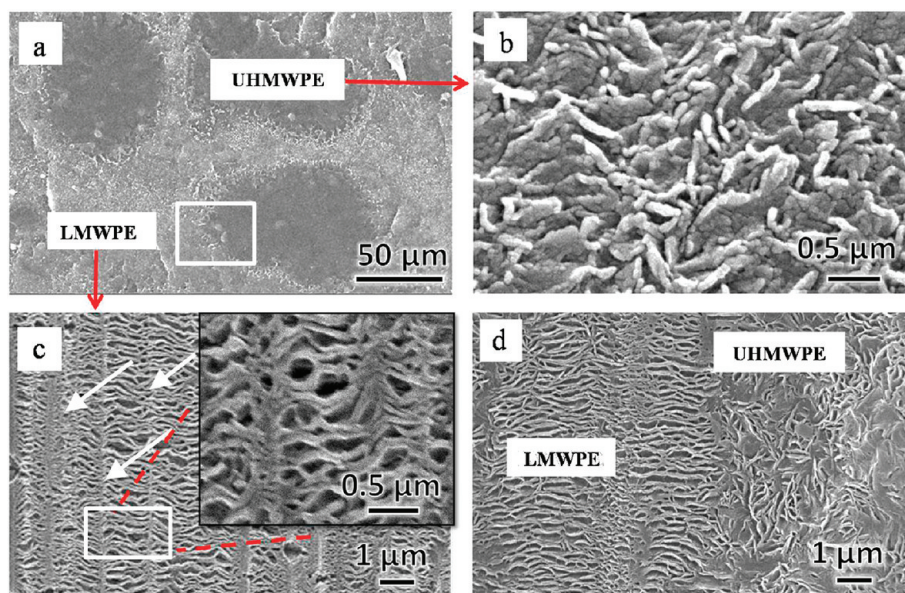

Figure 4. SEM images of (a) outer layer of OSIM PE blend (the shear flow direction is vertical), cryo-fracture surface, (b) etched surface of UHMWPE phase, (c) LMWPE phase, and (d) intersection region.

commonly believed to enhance properties in the oriented direction. The ultimate tensile strength changes from 27.6 MPa for CM UHMWPE up to 78.4 MPa for OSIM PE blend along the flow direction and up to 33.5 MPa in its transverse direction. At the meantime, the impact strength (Figure 3d) of OSIM PE blend increases by 46 and 7% from 29.6 kJ/m^2 for CM UHMWPE up to 43.1 and 31.8 kJ/m^2 for OSIM PE blend in the direction parallel and vertical to the shear flow,

respectively. An increased Young's modulus (Figure 3c) is also observed from 1.25 GPa for CM UHMWPE up to 1.74 and 1.62 GPa for OSIM PE blend in the two directions, respectively. The elongation at break (Figure 3b) of OSIM PE blend in both directions shows a decrease, from 211.4% for CM UHMWPE to 68.7% parallel to the shear flow direction and 49.3% in the transverse direction. Actually, the elongation of

1524

dx.doi.org/10.1021/am201752d | ACS Appl. Mater. Interfaces 2012, 4, 1521−1529

49.3% can completely meet the normal requirement for joint implants.[43]

The wear rate of the OSIM PE blend in the direction parallel (6.1 mg/MC) and vertical to the shear flow (7.8 mg/MC) is both reduced as comparison to the control sample of CM UHMWPE (8.1 mg/MC) (Figure 3e). The OSIM PE blend along both the directions exhibits comparable fatigue crack propagation resistance to CM UHMWPE (Figure 3f).

In summary, the comprehensive performance of the OSIM PE blend is significantly improved compared to the control sample of the CM UHMWPE. Specifically speaking, the enhanced ultimate tensile strength can allow the in vivo joint implants to endure stronger tensile loading, and improved impact strength of OSIM PE blend is more beneficial for stress transfer through plastic deformation, thus extending the use of this kind of joint implants to younger and more active patients. Moreover, the satisfying wear and fatigue crack propagation resistance can help decrease risk of peri-prosthetic osteolysis and fatigue fracture of total joint implants, respectively, prolonging the longevity of arthroplasty. Inspiringly, it is indeed the first time to successfully process the PE blend with significantly improved comprehensive performance in comparison with traditional CM UHMWPE by utilizing conventional polymer processing methods.

To elucidate the superior properties of the OSIM PE blend, we carefully examined its microstructure. Morphology of outer layer of OSIM PE blend is exhibited in Figure 4 and that of inner layer is displayed in Figure S4 in the Supporting Information. Figure 4a shows the cryo-fracture surface of the OSIM PE blend. One can clearly observe individual UHMWPE particles with their edges fused with LMWPE matrix (Figure 4a). The fracture occurs in the central region of most individual UHMWPE particles, not around the interfaces between LMWPE and UHMWPE, suggesting a strong interfacial adhesion.

To further ascertain the superstructure, we etched away the amorphous phase in cryo-fracture surface. One can easily indentify that a large amount of oriented crystals, i.e., shish-kebab superstructure, exists in the LMWPE phase (Figure 4c), in particular, many shish-kebab crystals connected by adjacent kebabs penetrate into each other, forming an interlocking state (see the inset picture of Figure 4c), which could be considered as the formation of interlocking shish-kebab superstructure. In the individual UHMWPE particles, there are only randomly arranged crystalline lamellae (Figure 4b). In the border region of LMWPE and UHMWPE phases, the edges of their separate crystalline lamellae intersect each other and thus are hardly distinguished (Figure 4d), whereas in the CM UHMWPE, only randomly distributed crystalline lamellae of UHMWPE can be observed, which is the same as the individual UHMWPE particles in the OSIM PE blend, and is not exhibited here for brevity.

The interlocking shish-kebab superstructure existing in LMWPE phase is probably the most obvious structural difference between OSIM PE blend and CM UHMWPE. Considering the superstructure of these two samples, we can definitely draw the conclusion that the loss of mechanical properties of UHMWPE caused by addition of LMWPE is offset by designing and manipulating the superstructure of the UHMWPE/LMWPE blend.

The crystal structure was indirectly verified by melting behavior, as shown in Figure 5. One can clearly observe two peaks in the DSC heating curves of the outer layer of OSIM PE
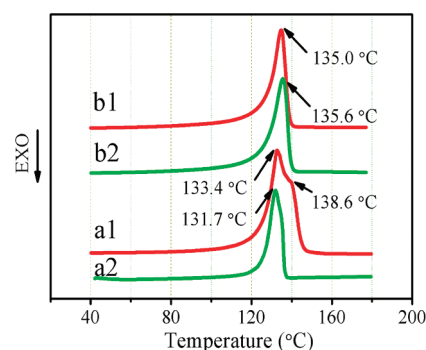

Figure 5. DSC heating curves of outer and inner layers of (a1, a2) OSIM PE blend and (b1, b2) CM UHMWPE.

blend, indicating two types of crystal morphology in this layer (Figure 5, curve a1). The lower temperature peak at 133.4 °C is ascribed to the melting of normal lamellae, whereas the higher one at 138.6 °C can be considered as the melting of shish-kebab superstructure.[44] In contrast, only one peak at 131.7 °C is observed in the inner layer (Figure 5, curve a2), which is lower than those two melting temperatures in the outer region. This result is well-consistent with the SEM observation that the shish-kebab structure only exists in the outer layer, but randomly distributed lamellae in the inner layer of OSIM PE blend. For CM UHMWPE, only one melting peak appears in the DSC heating curves of both layers (Figure 5, curves b1 and b2), thus the same crystal structure exists in the whole sample. The crystallinity estimated from the DSC curves is listed in Table 1. Compared to the CM UHMWPE, a significant

Table 1. Crystallinity (%) of OSIM PE Blend and CM UHMWPE

group	crystallinity (%)
OSIM PE blend	79.3
CM UHMWPE	56.7

increase in crystallinity appears for the OSIM PE blend. The mechanical properties and fatigue strength of UHMWPE depend directly on the content of the crystalline domains. A high crystallinity is favorable to enhancing fatigue strength.[45] The improved mechanical properties may be ascribe to the formation of interlocking shish-kebab superstructure and the great increase in crystallinity. As shown in Table S1 in the Supporting Information, crystallinity of common injection molded (CIM) PE blend without shear is 72.9%, which is very close to the value of OSIM PE blend. However, the increase in mechanical properties of CIM PE blend is much smaller than those of OSIM PE blend (see Table S1 in the Supporting Information). Thus, the formation of rich interlocking shish-kebab superstructure is considered to play a crucial role in the improved mechanical properties.

To deeply understand the structure−property relationship, we also employed 2D-WAXS and 2D-SAXS to determine the crystal structure. The selected 2D-WAXS patterns of the outer and inner layers are shown in Figure 6. The diffraction reflections from inner to outer circles are assigned to the (110) plane and (200) plane of PE orthorhombic crystals, respectively. For the OSIM PE blend, two focused arc-like strong diffraction reflections in the outer layer (Figure 6a1) are attributed to the existence of oriented crystalline super-structures.[47] However, the arc-like diffractions are absent in
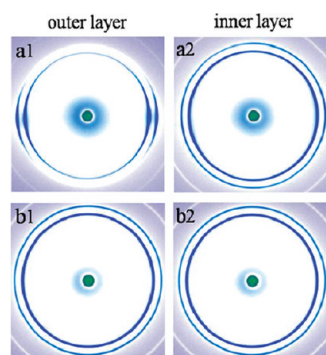
Figure 6. 2D-WAXS patterns of outer and inner layers of (a1, a2) OSIM PE blend and (b1, b2) CM UHMWPE.

the inner layer, instead, the nearly homogeneous circle reflection appears (Figure 6a2), indicating a random distribution of crystalline lamellae. The above phenomenon is also well-coordinated with the SEM observation. It is worth noticing that only isotropic diffraction circles are observed in the CM UHMWPE (Figure 6b1, b2), which is similar to the diffractograms of CIM PE blend exhibited in Figure S5 in the Supporting Information. The degree of orientation is calculated as listed in Table 2. The crystals in the CM UHMWPE are

Table 2. Degrees of Orientation of Various Layers of CM UHMWPE and OSIM PE Blend Obtained by 2D-WAXS

degrees of orientation	OSIM PE blend	CM UHMWPE
outer layer	0.950	0
inner layer	0.281	0

absolutely isotropic, whereas the degree of orientation is 0.950 and 0.281 in the outer and inner layers of the OSIM PE blend, respectively. These results substantially testify that the oriented structure effectively engenders with the help of flow field in the OSIM processing, but hardly forms in such static processing technologies as compression molding.

Figure 7 shows selected 2D-SAXS patterns of the outer and inner layers of two samples. For the OSIM PE blend samples, both equatorial streak and meridional scattering maxima appear at the out layer (Figure 7). The equatorial streak verifies the existence of a shish structure parallel to the flow direction.[46] The meridional scattering maxima refers to the kebabs, which grow perpendicularly to the shish axis through the folded-chain
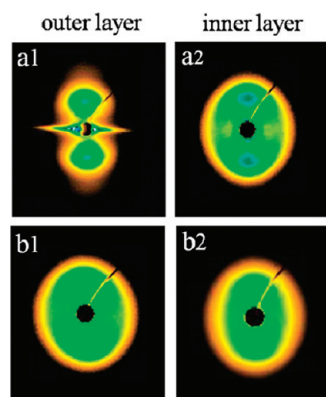

Figure 7. Selected 2D SAXS images of outer and inner layers of OSIM PE blend (a1, a2) and CM UHMWPE (b1, b2).

crystallization process. However, the inner layer exhibits the weak and broad meridional maximum without any signal of equatorial streak, implying formation of only less oriented arrangement of PE lamellae. In contrast, for the CM UHMWPE samples, apart from no trace of equatorial streak, the meridional scattering maxima is very obscure in both layers, which suggests absence of shish-kebab or oriented structure. Figure 8 shows Lorentz-corrected intensity profiles of circularly
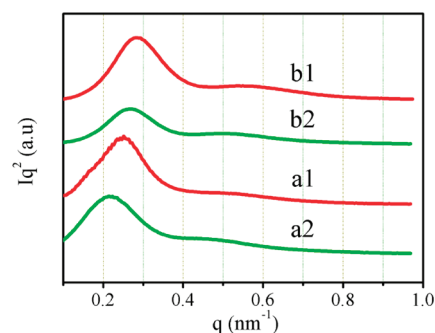

Figure 8. Lorentz-corrected SAXS intensity profiles of outer and inner layers of (a1, a2) OSIM PE blend and (b1, b2) CM UHMWPE.

integrated 2D SAXS patterns of the outer and inner layers. Using Bragg's law, the long spacing (L) was estimated from the peak position, as listed in Table 3. The OSIM PE blend samples

Table 3. Long Spacing (L) at Different Depths of OSIM PE Blend and CM UHMWPE

long spacing (nm)	outer layer	inner layer
OSIM PE blend	25.0	29.3
CM UHMWPE	22.4	23.4

exhibit a large long period as compared to the CM UHMWPE samples, indicating larger thickness of PE lamellae or more perfect crystal structure. This is originated from the melt-shearing induced crystallization during OSIM processing.

■ DISCUSSION

We have demonstrated that applying oscillatory shear flow during injection molding triggered formation of oriented crystals and thus improved the mechanical properties of UHMWPE/LMWPE blend samples without the sacrifice of the excellent wear resistance of UHMWPE. More importantly, the interlocking shish-kebabs are largely generated, which accounts for the simultaneously improved comprehensive properties of OSIM PE blend samples in every direction. Thus, it is reasonable to believe that the OSIM PE blend has great potential as an advanced material for artificial joint implants.

In the OSIM process, a semicrystalline polymer factually undergoes a flow-induced nonisothermal crystallization process. It is well-known that shear flow can significantly affect the crystallization behaviors of semicrystalline polymers and further influence the final morphology and properties of the polymers.[47,48] During OSIM processing, as the mold-filling stage finishes, the reciprocating shear flow is imposed on the PE blend melt, hence, those PE chains with molecular weight higher than a critical value (M^*) can be extended and would crystallize into shish.[33] Addition of 2.0 wt % UHMWPE means a larger fraction of molecular chains above M^* in the LMWPE

1526

dx.doi.org/10.1021/am201752d | ACS Appl. Mater. Interfaces 2012, 4, 1521–1529
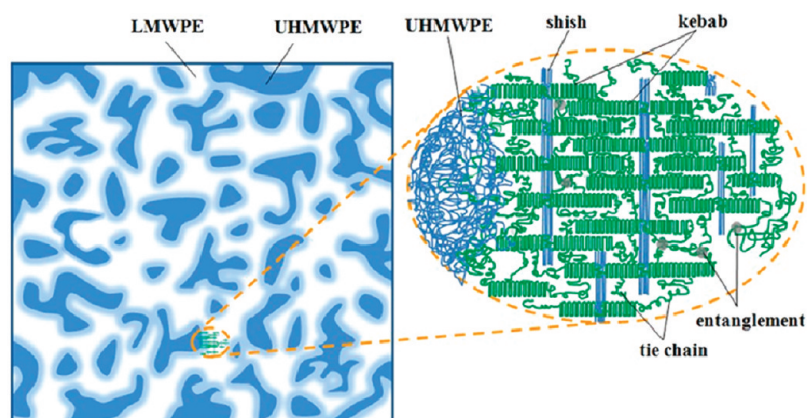
Figure 9. Schematic diagram of the OSIM PE blend morphology with interlocking shish-kebab self-reinforced superstructure.

phase, and forms more shish. The long chains have longer relaxation time, being beneficial to hold the orientation state, resulting in a more stable shish structure,[49] whereas the short ones remained coil, which are absorbed onto the shish, and crystallized in folded-chain lamellae, i.e., kebabs. Under the influence of shear, the growth of PE lamellae will align along the flow direction (Figure 4). In this work, the incorporation of additional UHMWPE into LMWPE can induce such a lot of shish. Also, many tie chains would be brought into the blend melt owing to the entanglements of UHMWPE. Considering the so much shish-kebab superstructure in a limited volume, the complicated linkage between shish or kebabs as well as the simultaneously existent oscillatory flow which can promote the adjacent PE lamellae intersect each other, we are substantially convinced the interlocking shish-kebab self-reinforced super-structure could be formed. The interlocking shish-kebab is a quite stable state, which properly endows the polymeric material with enhanced strength and facilitates stress transfer. The overall phase distribution of the OSIM PE blend and its internal structure containing local interlocking shish-kebab self-reinforced superstructure are schematically proposed in Figure 9. Meanwhile, the oscillation shear flow also has a positive effect on mixing the two-phase melt. On the one hand, UHMWPE and LMWPE probably exist with uniform distribution, which is conducive to keep the uniformity of bulk structure of the OSIM PE blend. On the other hand, the mixing effect prompts UHMWPE phase and LMWPE phase to penetrate into each other, thus making their interfacial adhesion strong enough (Figure 4).

It is worth noting that the shish-kebab superstructure mainly exists in the outer layers, which is attributed to the different cooling rate of the two layers. The surface of outer layer directly contacts the cool mold surface to cause a high cooling rate. Therefore, the flow-induced oriented threadlike nuclei are maintained to a large extent and then subsequently grow into shish-kebabs. However, in the interior region, the slow cooling leaves a sufficient time for oriented molecules (or network) to relax and consequently form spherulites without molecular orientation.

Due to the formation of plenty of shish-kebab superstructure, the ultimate tensile strength and Izod impact strength of the OSIM PE blend in the direction parallel to shear flow significantly improved compared to the CM UHMWPE (Figure 3a, 3d). Besides mechanical properties, wear is another important issue for the OSIM PE blend as a material for articulating surfaces. Common understanding of wear reduction

is based on a decrease in ductility by the cross-linking of chains in the amorphous phase.[50,51] The shish-kebab rigid structure in the OSIM PE blend improves its stiffness, and thus could efficaciously contribute to wear resistance, which is largely dependent on plastic deformation ability of the samples.[52] Furthermore, for the OSIM PE blend, the shish-kebab rigid structure is limited to the outer layer, which may serve as the articular surface of the implant, and the inner layer of the samples with less rigid structure could provide excellent ductility and plasticity. Combination of the complementary properties provides convincing evidence to substantiate the feasibility and rationality to control the formation of rigid structure under shear flow.

Fatigue resistance is closely related to the crystallinity of the OSIM PE blend as mentioned above. Injection molding of semicrystalline polymers is essentially a flow-induced non-isothermal crystallization process. On one hand, shear flow promoted significantly nuclei density and nucleating ki-netic.[53,54] On the other hand, viscous heat would be induced during distinct oscillatory shear flow, which left more time for PE melt to crystallize. The above two factors facilitate the uplift of crystallinity of the OSIM PE blend.

One major concern in the OSIM PE blend is whether the above properties in other directions deteriorate because of the existence of oriented structure. In this study, we found the comprehensive performance of the OSIM PE blend samples in the traverse direction is still superior to the CM UHMWPE sample. The remarkable result is definitely attributed to the existence of the interlocking shish-kebab self-reinforced super-structure and we speculate this interlocking state significantly enhances the interfacial adhesion between separate shish-kebab superstructure which is beneficial for the improvement of the stress transfer capability. The interlocking shish-kebab self-reinforced superstructure, which provides a tendency to homogenize properties of the samples in all directions, is indeed efficacious for performance improvement of the OSIM PE blend.

By utilizing the novel processing procedure, we have successfully fabricated the OSIM PE blend with superior properties through structure design. Considering all of these benefits mentioned above together, it is reasonable to believe that the OSIM PE blend has a highly potential application for joint implants. Furthermore, it is expected to significantly prolong the longevity of joint implants and effectively avoid the pain of patient during joint repair and replacement induced by implants failure.

CONCLUSIONS

We have successfully improved the comprehensive properties of OSIM PE blend through the formation of interlocking shish-kebab self-reinforced superstructure by applying shear flow during injection process. Shish-kebab self-reinforced super-structure endows PE blend samples with high strength, and its rigid character is conducive to the improvement of wear resistance along the direction of shear flow. Also, the increase in crystallinity plays an important role in improving the fatigue resistance of OSIM PE blend. Moreover, the interlocking state significantly enhances the interfacial adhesion between separate shish-kebab superstructure and also provides a tendency to homogenize properties of the samples in all directions which is indeed efficacious for performance improvement of the OSIM PE blend. Therefore, we have designed a novel PE blend, which has superb mechanical properties, high wear resistance and fatigue resistance far superior to CM UHMWPE. We are convinced of that this material is promising as a bearing surface for joint implants and all of the above benefits together may guarantee the longevity of OSIM PE blend as substitute for joint implants. The satisfying results in this work imply tailoring microstructure for improved performance is essential and beneficial for implant design and should gain more attention.

ASSOCIATED CONTENT

Ⓢ Supporting Information

Overall picture for Oscillation shear injection molding (OSIM) machine, 3D schematic illustration for the mold with an oscillation shear supplier, Complex viscosity and storage modulus of neat LMWPE and PE blend and SEM images of inner layer of OSIM PE blend are provided. This material is available free of charge via the Internet at http://pubs.acs.org.

AUTHOR INFORMATION

Corresponding Author

*E-mail: zmli@scu.edu.cn.

Notes

The authors declare no competing financial interest.

ACKNOWLEDGMENTS

REFERENCES

(1) Farrar, D. F.; Brain, A. A. *Biomaterials* **1997**, *18*, 1667−1685.
(2) Kurtz, S. M.; Muratoglu, O. K.; Evans, M.; Edidin, A. A. *Biomaterials* **1999**, *20*, 1659−1688.
(3) Harris, W. H. *Clin. Orthop. Relat. Res.* **1995**, *311*, 46−53.
(4) Willert, H. G.; Bertram, H.; Buchhorn, G. H. *Clin. Orthop. Relat. Res.* **1990**, *258*, 95−107.
(5) Muratoglu, O. K.; Merrill, E. W.; Bragdon, C. R.; O'Connor, D. O.; Hoeffel, D.; Burroughs, B.; Jasty, M.; Harris, W. H. *Clin. Orthop. Relat. Res.* **2003**, *417*, 253−262.
(6) McKellop, H.; Shen, F. W.; Lu, B.; Campbell, P.; Salovey, R. *J. Orthop. Res.* **1999**, *17*, 157−167.
(7) Digas, G.; Kärrholm, J.; Thanner, J.; Herberts, P. *Acta Orthop.* **2007**, *78*, 746−754.
(8) Costa, L.; Luda, M. P.; Trossarelli, L.; Brach del Prever, E. M.; Crova, M.; Gallinaro, P. *Biomaterials* **1998**, *19*, 659−668.
(9) Gomoll, A.; Wanich, T.; Bellare, A. *J. Orthop. Res.* **2002**, *20*, 1152−1156.
(10) Baker, D. A.; Bellare, A.; Pruitt, L. *J. Biomed. Mater. Res.* **2003**, *66A*, 146−154.
(11) Ries, M. D.; Pruitt, L. *Clin. Orthop. Relat. Res.* **2005**, *440*, 149−156.
(12) Simis, K. S.; Bistolfi, A.; Bellare, A.; Pruitt, L. *Biomaterials* **2006**, *27*, 1688−1694.
(13) Oral, E.; Wannomae, K. K.; Hawkins, N.; Harris, W. H.; Muratoglu, O. K. *Biomaterials* **2004**, *25*, 5515−5522.
(14) Fu, J.; Ghali, B. W.; Lozynsky, A. J.; Oral, E.; Muratoglu, O. K. *Polymer* **2010**, *51*, 2721−2731.
(15) Kurtz, S. M. *The UHMWPE Handbook: Ultra-High Molecular Weight Polyethylene in Total Joint Replacement*; Elsevier Academic Press: San Diego, CA, 2004.
(16) Muratoglu, O. K.; Bragdon, C. R.; O'Connor, D. O.; Jasty, M.; Harris, W. H.; Gul, R.; McGarry, F. *Biomaterials* **1999**, *20*, 1463−1470.
(17) Wittmann, J. C.; Lotz, B. *Polym. Sci., Polym. Phys. Ed.* **1985**, *23*, 205−226.
(18) Oral, E.; Rowell, S. L.; Muratoglu, O. K. *Biomaterials* **2006**, *27*, 5580−5587.
(19) Tower, S. S.; Currier, J. H.; Currier, B. H.; Lyford, K. A.; Van Citters, D. W.; Mayor, M. B. *J. Bone Joint Surg. Am.* **2007**, *89*, 2212−2217.
(20) Sui, G.; Zhong, W. H.; Ren, X.; Wang, X. Q.; Yang, X. P. *Mater. Chem. Phys.* **2009**, *115*, 404−412.
(21) Fouad, H.; Elleithy, R. *J. Mech. Behav. Biomed. Mater.* **2011**, *4*, 1376−1383.
(22) Chen, J.; Yang, W.; Yu, G. P.; Wang, M.; Ni, H. Y.; Shen, K. Z. *J. Mater. Process. Technol.* **2008**, *202*, 165−169.
(23) Lim, K. L. K.; Mohd Ishak, Z. A.; Ishiaku, U. S.; Fuad, A. M. Y.; Yusof, A. H.; Czigany, T.; Pukanszky, B.; Ogunniyi, D. S. *J. Appl. Polym. Sci.* **2005**, *97*, 413−425.
(24) Galetz, M. C.; Blaβ, T.; Ruckdäschel, H.; Sandler, J. K. W.; Altstädt, V.; Glatzel, U. *J. Appl. Polym. Sci.* **2007**, *104*, 4173−4181.
(25) Matsuba, G.; Sakamoto, S.; Ogino, Y.; Nishida, K.; Kanaya, T. *Macromolecules* **2007**, *40*, 7270−7275.
(26) Kakiage, M.; Yamanobe, T.; Komoto, T.; Murakami, S.; Uehara, H. *Polymer* **2006**, *47*, 8053−8060.
(27) Fukushima, H.; Ogino, Y.; Matsuba, G.; Nishida, K.; Kanaya, T. *Polymer* **2005**, *46*, 1878−1885.
(28) Cao, W.; Wang, K.; Zhang, Q.; Du, R. N.; Fu, Q. *Polymer* **2006**, *47*, 6857−6867.
(29) Wang, K.; Chen, F.; Zhang, Q.; Fu, Q. *Polymer* **2008**, *49*, 4745−4755.
(30) Hsiao, B. S.; Yang, L.; Somani, R. H.; Avila-Orta, C. A.; Zhu, L. *Phys. Rev. Lett.* **2005**, *94*, 117802−1−117802−4.
(31) Zuo, F.; Keum, J. K.; Yang, L.; Somani, R. H.; Hsiao, B. S. *Macromolecules* **2006**, *39*, 2209−2218.
(32) Seki, M.; Thurman, D. W.; Oberhauser, J. P.; Kornfield, J. A. *Macromolecules* **2002**, *35*, 2583−2594.
(33) Somani, R. H.; Hsiao, B. S.; Nogales, A.; Srinivas, S.; Tsou, A. H.; Sics, I.; Balta-Calleja, F. J.; Ezquerra, T. A. *Macromolecules* **2000**, *33*, 9385−9394.
(34) Jerschow, P.; Janeschitz-Kriegl, H. *Int. Polym. Process.* **1997**, *12*, 72−77.
(35) Vleeshouwers, S.; Meijer, H. E. H. *Rheol. Acta* **1996**, *35*, 391−399.
(36) Duplay, C.; Monasse, B.; Haudin, J. M.; Costa, J. L. *J. Mater. Sci.* **2000**, *35*, 6093−6103.
(37) Brady, J. M.; Thomas, E. L. *J. Mater. Sci.* **1989**, *24*, 3311−3318.
(38) Pornnimit, B.; Ehrenstein, G. W. *Adv. Polym. Technol.* **1991**, *11*, 91−98.
(39) Prox, M.; Pornnimit, B.; Varga, J.; Ehrenstein, G. W. *J. Therm. Anal.* **1990**, *36*, 1675−1684.
(40) Keum, J. K.; Zuo, F.; Hsiao, B. S. *Macromolecules* **2008**, *41*, 4766−4776.
(41) Na, B.; Zhang, Q.; Fu, Q.; Zhang, G.; Shen, K. Z. *Polymer* **2002**, *43*, 7367−7376.

(42) Picken, S. J.; Aerts, J.; Visser, R.; Northolt, M. G. *Macromolecules* **1990**, *23*, 3849−3854.

(43) Oral, E.; Muratoglu, O. K. *Nucl. Instrum. Meth. Phys. Res., Sect. B* **2007**, *265*, 18−22.

(44) Yang, J. H.; Wang, C. Y.; Wang, K.; Zhang, Q.; Chen, F.; Du, R. N.; Fu, Q. *Macromolecules* **2009**, *42*, 7016−7023.

(45) Oral, E.; Malhi, A. S.; Muratoglu, O. K. *Biomaterials* **2006**, *27*, 917−925.

(46) Yang, L.; Somani, R. H.; Sics, I.; Hsiao, B. S.; Kolb, R.; Fruitwala, H.; Ong, C. *Macromolecules* **2004**, *37*, 4845−4859.

(47) Janeschitz-Kriegl, H.; Ratajski, E.; Stadlbauer, M. *Rheol. Acta* **2003**, *42*, 355−364.

(48) Stadlbauer, M.; Janeschitz-Kriegl, H.; Eder, G.; Ratajski, E. *J. Rheol.* **2004**, *48*, 631−639.

(49) Nogales, A.; Hsiao, B. S.; Somani, R. H.; Srinivas, S.; Tsou, A. H.; Balta-Calleja, F. J.; Ezquerra, T. A. *Polymer* **2001**, *42*, 5247−5256.

(50) Muratoglu, O. K.; Bragdon, C. R.; O'Connor, D. O.; Jasty, M.; Harris, W. H. *J. Arthroplasty* **2001**, *16*, 149−160.

(51) McKellop, H.; Shen, F. W.; Lu, B.; Campbell, P.; Salovey, R. *J. Orthop. Res.* **1999**, *17*, 157−167.

(52) Edidin, A. A.; Pruitt, L.; Jewett, C. W.; Crane, D. J.; Roberts, D.; Kurtz, S. M. *J. Arthroplasty* **1999**, *14*, 616−627.

(53) Janeschitz-Kriegl, H.; Ratajski, E. *Polymer* **2005**, *46*, 3856−3870.

(54) Janeschitz-Kriegl, H. *Macromolecules* **2006**, *39*, 4448−4454.